High Speed Jet Noise

Victor F. Kopiev
Central Aerohydrodynamics Institute (TsAGI), Acoustic Division
105005 Moscow, Radio str.17, Russia

vkopiev@mx.iki.rssi.ru

INTRODUCTION

Recent advances in computational aerodynamics have encouraged the attempts of direct numerical simulation of the aero-acoustic processes in supersonic jets. However, despite significant efforts being spent, this approach has not given any definite results in solving the problem up to now. The main obstacle is the wide range of spatial and temporal scales which have to be accounted for in order to fully solve aero-acoustic problems. This range ensures that the task still lies outside the limits of modern computational capabilities for high Reynolds number. This is why there is much current interest directed at search of mechanisms which are the main source of acoustical radiation. The relative input of each mechanism is not clear as yet, though it is indeed necessary to know a concrete radiation mechanism for developing the methods of noise control, numerical methods of noise prediction etc.

It is now generally accepted that one of the main mechanisms of acoustic radiation in a supersonic jet can be identified with packets of instability waves propagating downstream within the mixing layer of the jet [1]. This follows from the generally accepted assumption [2] that supersonic jet noise is generated by large-scale turbulence which, in turn, can be represented as a sum of spatially developing waves. Tam's method is based on two fundamental principles: 1) the main part of mixing noise is radiated by instability waves evolving downstream from the nozzle edge; 2) near the nozzle edge the initial amplitudes of instability waves of all the harmonics, in the range of Strouchal numbers being of interest, are the white noise. Thus, the unknown parameter of the theory is only one constant which is a power of the white noise. This constant within the limits of such an approach can be obtained from the experiment data. Assumption (1) is based on the idea that the instability wave as the most growing one must significantly increase in its evolution to the zone of maximum. It substantially exceeds other disturbances in this zone and is the principal and effective radiation source if its velocity remains supersonic (Fig.1). Moreover instability wave despite increasing continues to be wave packet in zone of maximum that means nonlinear rolling up of shear layer typical for subsonic jet does not begin. Assumption (2) is based on ideas on the absence of the characteristic length scale near the nozzle edge where the instability waves originate.

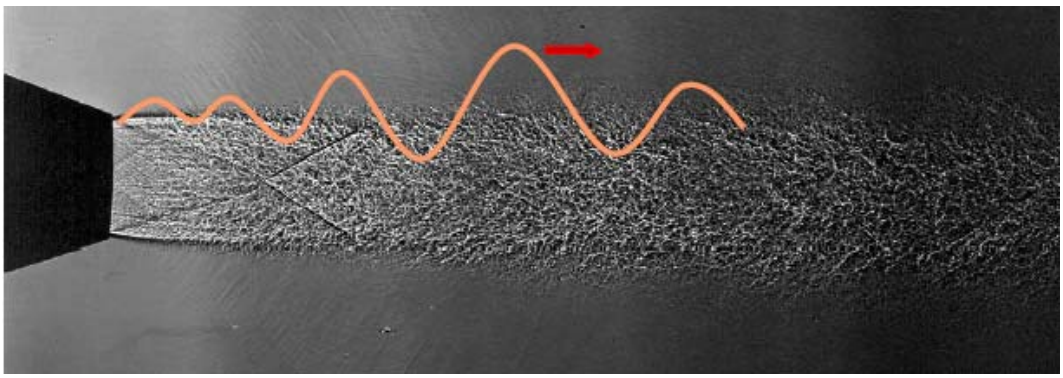

Figure 1: Supersonic jet and scheme of instability wave packet

Kopiev, V.F. (2008) High Speed Jet Noise. In *Advances on Propulsion Technology for High-Speed Aircraft* (pp. 13-1 – 13-26). Educational Notes RTO-EN-AVT-150, Paper 13. Neuilly-sur-Seine, France: RTO. Available from: http://www.rto.nato.int.

It should be noted that there are alternative approaches for supersonic jet prediction [3] recently further developed in [4]. Therefore the answers, which are "vitally important", are: do the instability waves really exist and radiate noise? Does the instability wave mechanism dominate each other? Do the amplitudes of instability waves smoothly distributed near orifice or some scales of disturbances are dominated, etc. It is clear that the knowledge about this mechanism and its dynamic features is the first and necessary condition of the elaboration of noise control strategyand has a direct importance for the flight vehicles future elaboration. Along with the experimental validation available, obtained for St=0.2 previously [5], the direct validation of the instability wave theory in the round jet was recently realized by azimuthal decomposition technique [6] in the region of Sh~0.1-0.35 to be sure that this mechanism really exists and dominates any other. Azimuthal modes are directly under consideration in Tam theory and their relative amplitudes could give careful instrument for theory development and unique possibility of comparing the theory and its principal concepts with the results of the experiments.

Supersonic jet noise consists of three main components. They are the turbulent mixing noise, the broadband shock associated noise and the screech tones. The latter two noise components are generated only when the jet is imperfectly expanded and a shock cell structure is formed in the jet plume. This lecture considers perfectly expanded jets and turbulent mixing noise alone.

Thus in the present work we consider the main principles of Tam instability wave theory for mixing noise and new approach to verification this theory on the basis of the experimental data obtained with the use of the azimuthal decomposition technique (see review of the problem in [7]), Fig.2. In the first part of the work we consider the instability wave concept for the simplest 2D shear layer. In the second part the looking over the Tam's theory details was conducted. This analysis gives the main background for comparison with experiment. In the third experimental part of this work the method of azimuthal decomposition, which helps to measure directly the azimuthal harmonic amplitudes and directivities, is used for the well-shaped convergent-divergent axisymmetrical nozzle designed for exit Mach number M=2. The method is used for careful acoustic measurements.

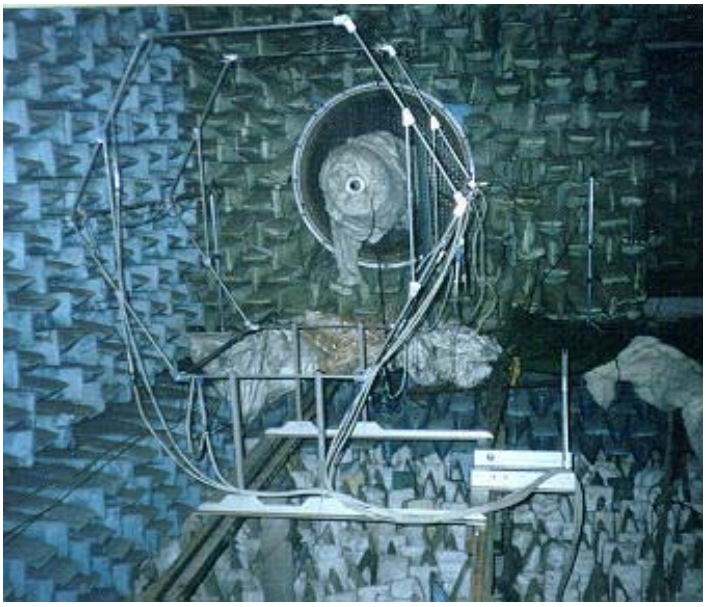

Figure 2. Microphone array in anechoic chamber for azimuthal decomposition technique

A comparison between the theory predictions and the measurement data shows that for all azimuthal harmonics n = 0, 1 and 2, which contribute the main part to the jet noise, the theory predictions are in

agreement with measurement data. It concerns the directivity of sound radiation, frequency dependence of radiation peak and amplitude scales of sound radiation for different harmonics in frequency ranges. It means that the experimental results have confirmed two main hypothesis of Tam's theory: i) the main source of sound in supersonic fully expanded jet are the instability waves; ii) the instability waves have an amplitude of the same order in the region of their origination in wide frequency range and for different harmonics. Therefore the instability waves could be considered as objects for direct noise control in supersonic jet.

AZIMUTAL MODE MEASUREMENTS

We briefly discuss in this chapter the measurements of supersonic round cold jet noise following the paper [8], where the method of azimuthal decomposition for noise measurements was firstly used. This technique gives a possibility of measuring the noise of each azimuthal mode separately. In experiment the mixing noise of supersonic cold jet from convergent-divergent conical nozzles of design Mach number M=2.0 was studied. The experimental program consisted of measuring the azimuthal mode intensity in different frequency ranges by a six-microphone array. The results for the special "well shape nozzle" to measure the mixing noise only is considered to the end of the lecture.

The microphone array moves along jet axis z from 0 to 250 cm covering the cylindrical surface around the jet. The nozzle orifice position corresponds to the section z=50 cm. The scheme of the experiment is presented in Fig. 3. We present only low frequency results for jet noise azimuthal decompositions up to St~0.3. The more careful discussion of the problem will be presented below.

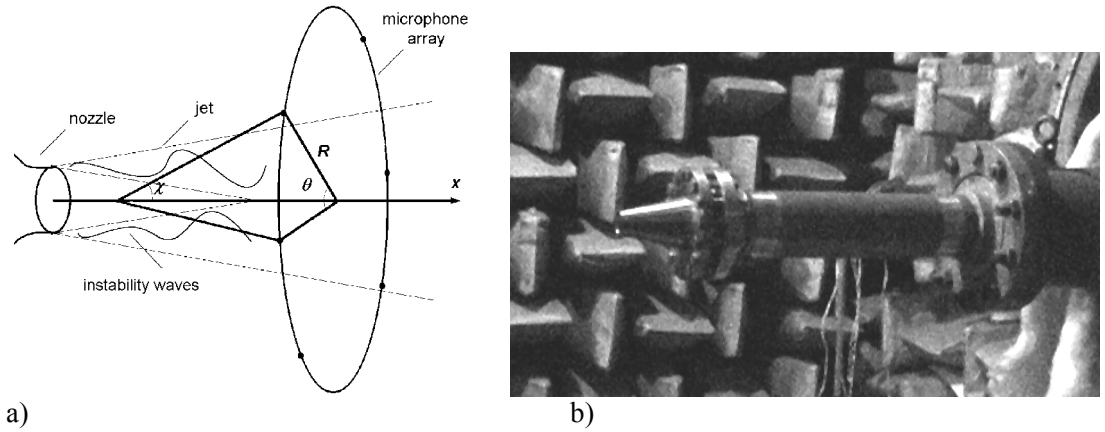

Figure 3. Scheme of experiment (a); supersonic nozzele (b).

Fig.4 presents the powers of four azimuthal modes $a_0^2, a_1^2, a_2^2, a_3^2$ (where subscript corresponds to the number of azimuthal harmonic) as the result of azimuthal noise decomposition. We see that only axisymmetric radiation dominates in the low frequency range, the first mode appears only for Sh~0.2. So, only a few first azimuthal modes give a contribution to the round jet noise. The second and the third modes are absent in this range. The supersonic jet noise directivity has a strong maximum in downstream direction. Prediction of supersonic jet noise based on Tam's theory presents on Fig.5. This regime with intensified axisymmetrical mode was used for directivity comparison in [6].

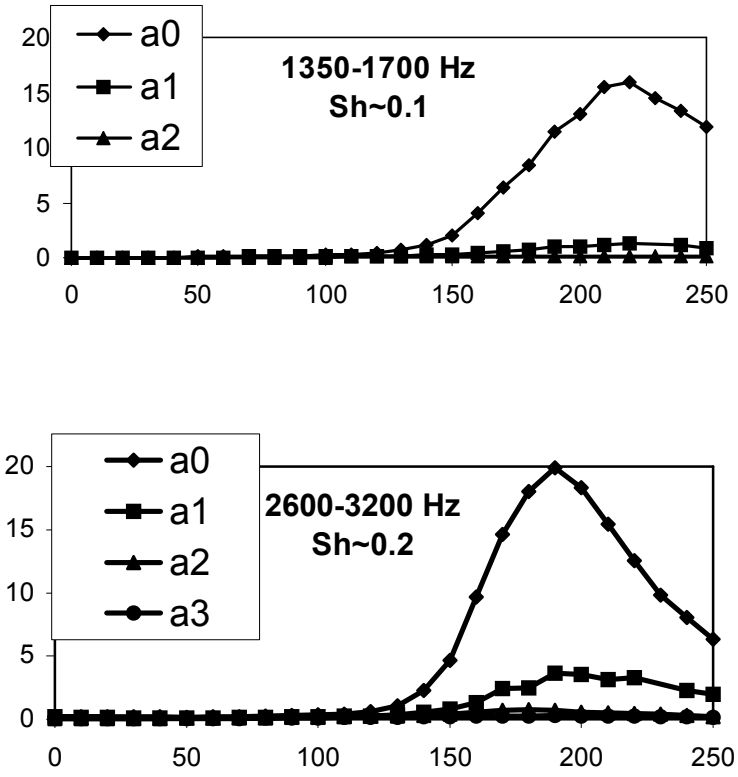

Figure 4. Directivity of azimuthal modes in two frequency ranges: a) Sh~0.1, domination of axisymmetrical mode; b) Sh~0.2, appearing first (*n*=1) azimuthal mode in far field.

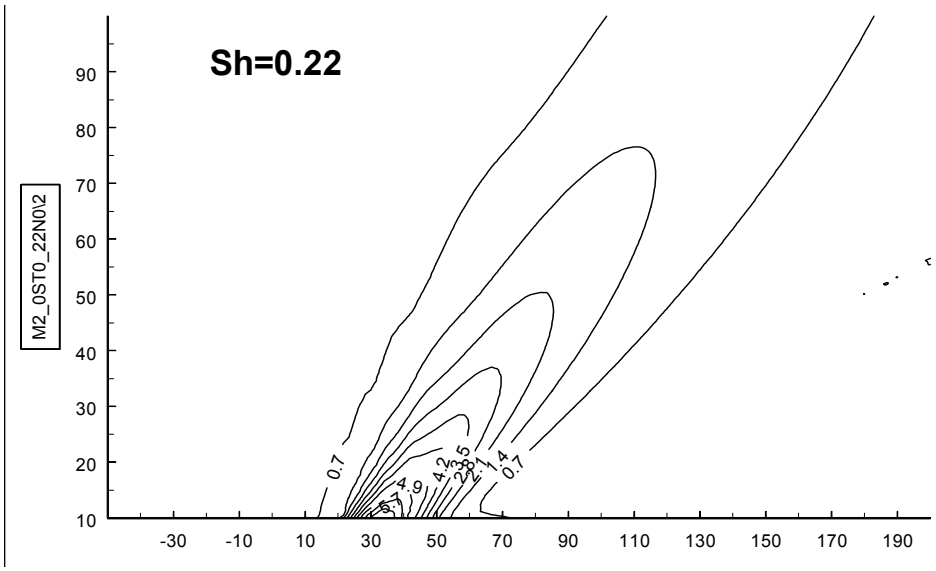

Figure 5. The sound pressure levels created by instability wave packet in the near field of supersonic cold jet at *M*=2, *St*=0,22 for azimuthal harmonic *n*=0.

Since the instability waves are the main element of the theory we consider their main features in simplest situations in some details.

INSTABILITY WAVE PROBLEM

Vortex sheet waves

Vortex sheet model corresponds to the initial part of shear layer near the nozzle. This part of shear layer is one of the most important one due to it strong instability and great sensibility to the outer disturbances. The problem of designing the advanced propulsion system requires the high velocity jets of complex configuration to be investigated. For such jets the representation of the shear layer in the form of vortex sheet is a substantial simplification. We will discuss some approach to the instability wave concept, restricting ourselves by 2D problem and begin from the eigen solution for the vortex sheet separated the uniform flow from the surrounding gas [9-11].

Consider the simplest model of the mixing layer, i.e. a vortex sheet model. Let (x, y) be Cartesian system of coordinates with the x-axis oriented along the main flow. In the region I ($y > 0$) where the fluid is at rest and in the region II ($y < 0$) of the uniform flow with the velocity V_0, the disturbances of the potential φ are governed by the wave equation and by the convective wave equation, respectively

$$\frac{\partial^2 \varphi_1}{\partial t^2} - \Delta\, \varphi_1 = 0, \qquad y > 0 \tag{1}$$

$$\frac{D^2 \varphi_2}{D t^2} - \Delta \varphi_2 = 0 \qquad y < 0, \tag{2}$$

$$\frac{D}{Dt} \equiv \frac{\partial}{\partial t} + V_0 \frac{\partial}{\partial x}$$

At the vortex sheet $y = 0$ the boundary conditions of pressure continuity

$$\frac{\partial \varphi_1}{\partial t} = \frac{D \varphi_2}{D t} \tag{3a}$$

and of boundary displacement continuity

$$\frac{D}{D t} \frac{\partial \varphi_1}{\partial y} = \frac{\partial}{\partial t} \frac{\partial \varphi_2}{\partial y}. \tag{3b}$$

are to be fulfilled.

For disturbances of $\exp(-ikct - i\alpha x)$ type (c is the sound velocity) the solutions of Eqs. (1), (2) are as follows: $\varphi_1 \sim e^{-\gamma y}, \varphi_2 \sim e^{\beta y}$, where functions γ and β are the following:

$$\gamma = \sqrt{\alpha^2 - k^2}, \quad \beta = \sqrt{(1 - M_0^2)\alpha^2 - 2M_0 \alpha k - k^2}$$

The branches of the functions γ and β are selected according to the radiation condition: (i) the field must diminish at $y \to \pm\infty$ for every fixed t; (ii) the field must be produced by sources on the vortex sheet (causality).

It is easy to show that this condition at $k = k_1 + ik_2$ ($k_1 > 0$) is satisfied only by the solutions of the type of $k_2 > 0$, $\mathrm{Re}\ \gamma > 0$, $\mathrm{Re}\ \beta > 0$. The case $k_2 = 0$ is considered to be the limit of $k_2 \to +0$.

The dispersion relation determining the flow eigen-oscillations is as follows:

$$D_0(k,\alpha) = (k + \alpha M_0)^2\ \gamma + k^2\ \beta = 0 \tag{4}$$

The cuts of the function γ are realized from the branch points $\alpha = \pm k$ along the lines $\mathrm{Re}\,\gamma = 0$. The cuts of the function β are realized from the branch points $\alpha = \dfrac{k}{1-M_0}$, $\alpha = -\dfrac{k}{1+M_0}$ along the lines $\mathrm{Re}\,\beta = 0$, Fig. 6. The solution of equation (4) can be considered on four sheets of the Riemann surface of the function $D_0(k,\alpha)$: I. $\mathrm{Re}\,\gamma > 0, \mathrm{Re}\,\beta > 0$, II. $\mathrm{Re}\,\gamma < 0, \mathrm{Re}\,\beta > 0$, III. $\mathrm{Re}\,\gamma > 0, \mathrm{Re}\,\beta < 0$, IV. $\mathrm{Re}\,\gamma < 0, \mathrm{Re}\,\beta < 0$. We are interested in the solution on the first sheet only, where the branches of the functions γ and β are selected according to the radiation conditions said above, that is $\mathrm{Re}\,\gamma > 0, \mathrm{Re}\,\beta > 0$.

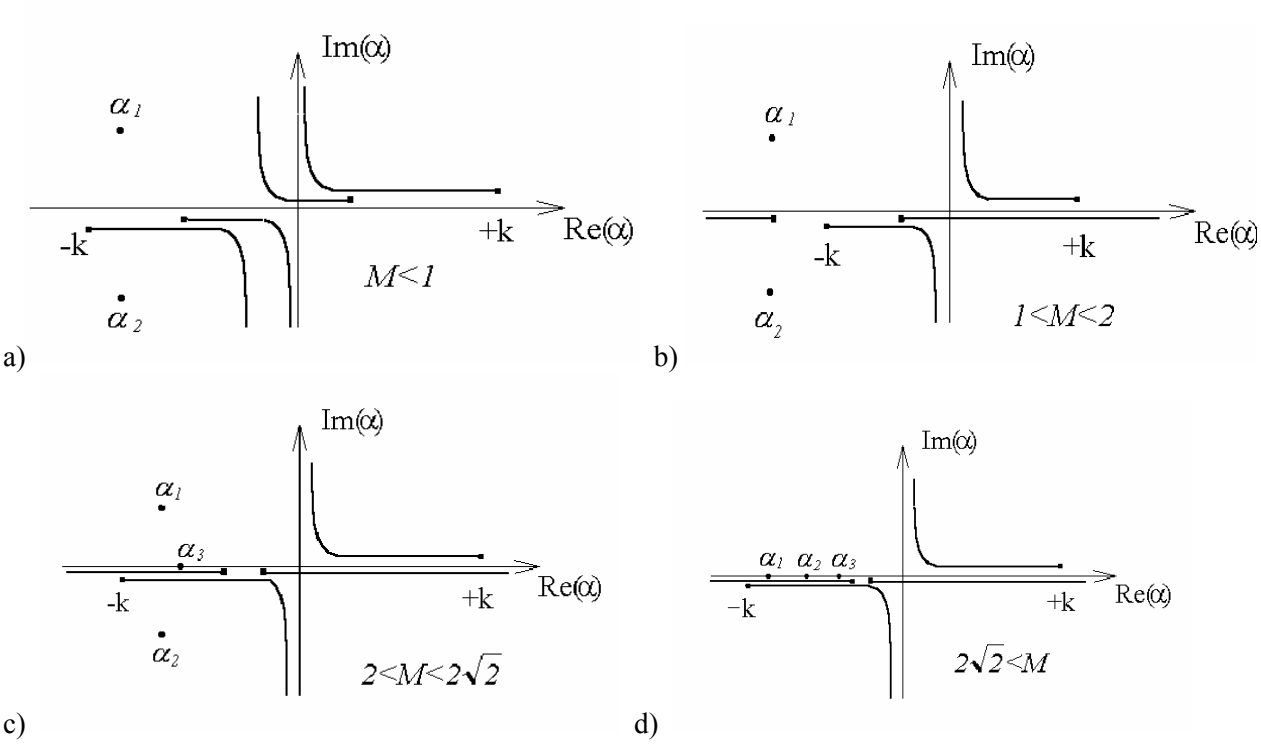

Figure 6. Possible positions of the roots α_i of the dispersion equation (4) on the complex plane of α according to M

The solutions of equation (4) in the complex plane α and at the real $k > 0$ depend on the flow Mach number [9-11]. At $M_0 < 2$ only two complex roots are available on the first sheet:

$$\frac{\alpha_{1,2}}{k} = \left[-\frac{M_0}{2} \mp i\sqrt{-\left(\frac{M_0^2}{4}+1\right) + \sqrt{1+M_0^2}} \right]^{-1} \tag{5a,b}$$

In this equation the upper sign (α_1-wave) corresponds to Kelvin-Helmholtz instability (Fig.6 a,b).

At $2 < M_0 < 2\sqrt{2}$ the complex roots (5) remain. Besides, the root

$$\frac{\alpha_3}{k} = -\frac{2}{M_0} \tag{6}$$

transfers from the second (third) sheet to the first (forth) one (Fig.6c). This root appearance is associated with overlap of the cuts of the functions γ and β.

At $M_0 \to 2\sqrt{2}$ two complex roots of the type of (5) approach the real axis. Thus at $M_0 > 2\sqrt{2}$ there are three real roots. Two of them are as follows:

$$\frac{\alpha_{1,2}}{k} = \left[-\frac{M_0}{2} \pm \sqrt{\left(\frac{M_0^2}{4} + 1 \right) - \sqrt{1 + M_0^2}} \right]^{-1} \tag{7}$$

The third root is defined by Eq.(6) (Fig.6d). Thus for the vortex sheet model the flow becomes steady at $M_0 > 2\sqrt{2}$ relative to 2-D disturbances. In such flow there are three neutrally stable waves determined by Eqs.(6), (7).

At very large M the expressions for the roots are simplified and are as follows:

$$\frac{\alpha_1}{k} = -1 + \frac{1}{2M_0{}^2} + O\left(M^{-3}\right), \quad \frac{\alpha_2}{k} = -\frac{1}{M_0 - 1} - \frac{1}{2M_0{}^2} + O\left(M^{-3}\right), \quad \frac{\alpha_3}{k} = -\frac{2}{M_0} \tag{8}$$

Thus the root α_1 displaces at large M along the real axis to the branch point of the function γ and the root α_2 displaces to the branch point of the function β.

To excite the eigen solutions (5)-(7) in initial value problem we must to consider the incidence field not orthogonal to them. For the scattering of plane acoustic wave these solutions are not excited [9-11]. Vortex sheet modes are excited in the more special problems where some non-uniformity is existed: (i) point source near the vortex sheet, (ii) plane wave scattering on the half plane, etc. Even in these problems to capture the instability pole with nonzero imaginary part some special technique based on causality principle is to be used. The limit regime as $t \to \infty$ could be realized for the convective instability system only [12-13]. The causality principle for such systems strongly differs from usual technique of small dissipation. The causal solution of initial value problem is based on Fourier transformation with complex k ($Im\, k \to \infty$) with subsequent analytical continuation $Im\, k \to 0$.

Point source near vortex sheet

Consider the sound source located over the vortex sheet $y_0 = L$ of $exp(-ik_0 ct)$ type switched on at $t > 0$ (initial value problem). There were many questions connected with statement of oscillation problem for the system of unconfined increase [14-16] which is incorrect according to Hadamar [17]. The other problem connects with using of Fourier transformation technique for unstable system. These problems were resolved following some ideas adopted from plasma physics and plasma instabilities [12-13]. Thus, the vortex sheet as oscillation system is supposed to be a realization of some system of confined increase with convective type of instability.

Consider the second problem in more details (Fig.7). The boundary conditions are formulated above (3a)-(3b).

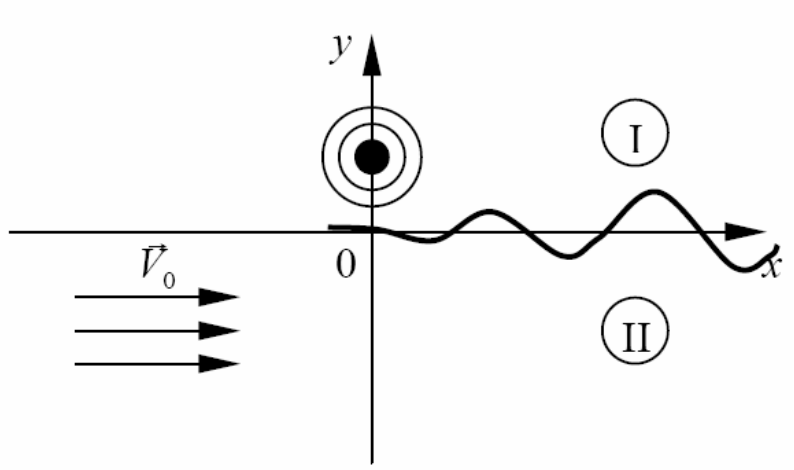

Figure 7. Sound source under the vortex sheet

For the Fourier transformation of the solution in the region I we obtain

$$\bar{\varphi}(\alpha, y) = \int_{-\infty}^{\infty} \varphi \exp(i\alpha x) dx$$

$$\varphi(x, y) = \frac{1}{2\pi} \int_C \frac{A(\alpha, k_0)}{\gamma} \exp(-\gamma(y + h) - i\alpha x) d\alpha \tag{9}$$

$$A(\alpha) = \frac{k_0^2 \beta - (k_0 + M\alpha)^2 \gamma}{k_0^2 \beta + (k_0 + M\alpha)^2 \gamma}, \tag{10}$$

Integrand in Eq. (9) includes the pole corresponding to the Kelvin-Helmholtz instability. The instability wave is equal to the residue in the denominator (10) at point (5b). If the contour C coincided with real axis it would not include the instability wave [18]. In correct solution the contour *C* is obtained from condition of analytical continuation from complex k_0 having large imaginary part to $Im\, k_0 \to 0$ (this procedure localize the position of the singularities in the α -plane, corresponding to the causal solution, Fig.8) [20-23].

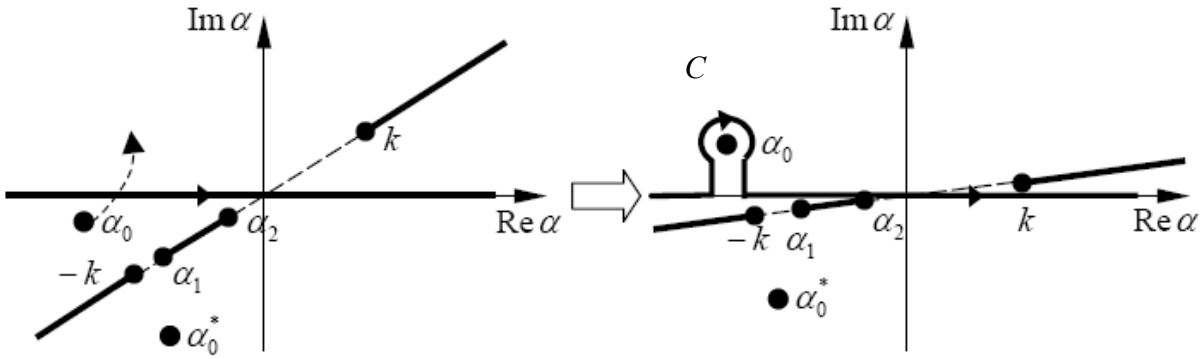

Figure 8 Localization of all peculiarities in $A(\alpha)$ (a) for the $Im\, k_0 \to \infty$, b) for $Im\, k_0 \to 0$.

Scattering of plane wave by semi-infinite screen

Suppose that plane wave is incident on the trailing edge from the supersonic stream (Fig.9). It is some image of instability wave generation in the turbulent jet due to the disturbances in the flow. We suggest that full Kutta-Zhukowsky condition is applied at the trailing edge. Reviews of Kutta conditions in different situations one could find in [24-25]. This problem is solved with the Wiener-Hopf technique.

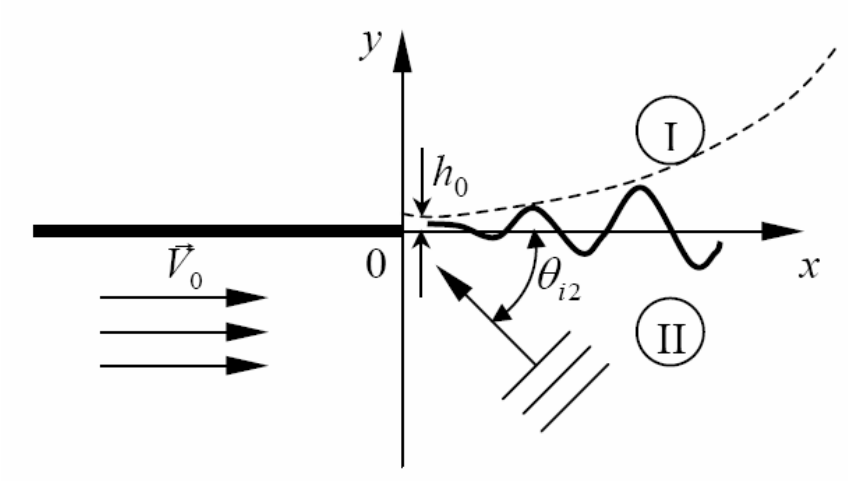

Figure 9. Plane wave incidence on the trailing edge

The capture of Kelvin-Helmholtz instability realized accordingly the same procedure (Fig.8b). The instability wave arises as the residue input in the pole α_0. Full solution contains the incident wave and diffraction field that along with instability wave satisfy the Kutta condition near the edge. Therefore the instability wave initial amplitude h_0 is determined by the incident wave properties only.

Instability wave in a mixing layer

For slowly divergent free shear flows such as 2D mixing layer the rate of spread ε could be considered as a small parameter (Fig.10). Then the shear layer thickness $H(\varepsilon x)$ is a function of slow variable εx. This selection of inner variables effectively ensures that the lowest-order solution is identical with that of the classical locally parallel-flow approximation.

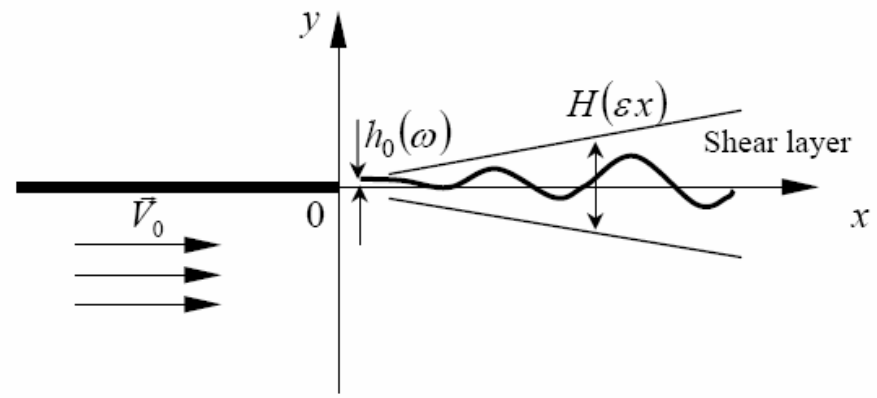

Figure 10. Plane wave incidence on the trailing edge with slowly divergent shear layer

Thus we suggest the instability wave has initial amplitude $h_0(\omega)$ near the edge where the shear layer is close to the vortex sheet. These amplitudes are free parameter in the theory considered later. We consider the initial amplitudes of the instability waves correspond to the diffraction of some incidence disturbances on the plate. The region near the edge gives start to instability wave packet. The amplitude of the packet grows exponentially in the downstream direction while shear layer is thin. After shear layer achieves some value the amplitude of wave packet begins to decrease. This evolution of the wave packet amplitude in downstream direction was considered carefully in the paper [26]. The global solution for noise radiated by wave packet was built there also.

TAM'S THEORY

Inside the jet the mean flow changes very slowly in the axial direction as compared to the radial direction. Therefore in the mixing layer of a supersonic jet the flow near the nozzle has a vortex sheet character and spreading rate of the jet in the downstream direction is very small so that this large disparity in the rate of spatial change in the two directions provides a natural small parameter for a multiple-scales expansion. Vortex sheet instability considered above gives the starting points for the instability wave generation and noise radiation in the supersonic jet. In addition 2D vortex sheet problem explains main difficulties which should be overcome to built the correct causal solution.

Governing Equations

Instability waves in the high-speed axisymmetrical jet and the acoustic radiation generated by these waves are considered. The linearized equations are used for their description. In addition, it is assumed that viscosity and heat conductivity play no significant role in the instability wave evolution.

The disturbances are described by the following equations

$$\frac{\partial \vec{v}}{\partial t}+\left(\vec{V}_0\nabla\right)\vec{v}+\left(\vec{v}\nabla\right)\vec{V}_0=-\frac{1}{\rho_0}\nabla p \tag{11}$$

$$\frac{\partial p}{\partial t}+\left(\vec{V}_0\nabla\right)p+\gamma P_0\,\nabla\vec{v}+\gamma\, p\nabla\vec{V}_0=0 \tag{12}$$

where $\vec{V}_0, P_0, \rho_0$ are mean flow velocity, pressure and density, $\vec{v}$, p are the disturbances of velocity and pressure, $\gamma=C_p/C_v$ is specific heat ratio. Equation (11) is the momentum equation, equation (12) is a combination of equations of continuity, energy and gas law.

The axial symmetry of the mean flow permits searching the solutions of the Eqs (11)-(12) in the form of separate azimuthal harmonics $exp\left(in\varphi\right)$ in cylindrical coordinates r,φ,z with z-axis directed along the jet. Assuming that the instability wave is generated by an external harmonic in time source we search for the solution in the form of $exp\left(-i\omega t\right)$. Then the equations (11)-(12) can be written in the form

$$-i\omega v^r+V\frac{\partial v^r}{\partial r}+U\frac{\partial v^r}{\partial z}+v^r\frac{\partial V}{\partial r}+v^z\frac{\partial V}{\partial z}+\frac{1}{\rho_0}\frac{\partial p}{\partial r}=0 \tag{13}$$

$$-i\omega v^\varphi+V\frac{\partial v^\varphi}{\partial r}+U\frac{\partial v^\varphi}{\partial z}+\frac{2}{r}V v^\varphi+\frac{in}{r^2\rho_0}p=0 \tag{14}$$

$$-i\omega v^z + V\frac{\partial v^z}{\partial r} + U\frac{\partial v^z}{\partial z} + v^r\frac{\partial U}{\partial r} + v^z\frac{\partial U}{\partial z} + \frac{1}{\rho_0}\frac{\partial p}{\partial z} = 0 \tag{15}$$

$$-i\omega p + V\frac{\partial p}{\partial r} + U\frac{\partial p}{\partial z} + \gamma p_0\left(\frac{1}{r}\frac{\partial}{\partial r}rv^r + inv^\varphi + \frac{\partial v^z}{\partial z}\right) + \gamma p\left(\frac{1}{r}\frac{\partial}{\partial r}rV + \frac{\partial U}{\partial z}\right) = 0 \tag{16}$$

where V and U are the r and z - components of the mean flow velocity, v^r, v^φ, v^z are the r, φ and z components of the velocity field disturbances.

The mean flow in the high-speed jet is characterized by a slow variation of parameters in the longitudinal direction, i.e. $\frac{\partial}{\partial z} = 0(\varepsilon)\frac{\partial}{\partial r}$, where $\varepsilon << 1$ is the small parameter. This permits searching the solution of the problem with the use of perturbation methods. In [27] the solution of this task using the method of matched asymptotic expansions is obtained. For this purpose the internal and the external regions were separated. The internal region is the jet interior and its vicinity and the external field is the whole space outside the jet.

Two approximations in terms of parameter ε are obtained in the internal region. The disturbances are written down as follows

$$p = A(s)\cdot\left[p_0(r,s) + \varepsilon\, p_1(r,s) + 0\left(\varepsilon^2\right)\right]\cdot \exp(i\,\phi) \tag{17}$$

where $s = \varepsilon z$ is the "slow" longitudinal coordinate, $\frac{\partial \phi}{\partial z} = \alpha(s)$, α is the local wave number. Thus, fast and slow variations relative to the longitudinal coordinate z are separated in the disturbances. In the main approximation, retaining the terms of $O(1)$ order we get from equations (3)-(6) a simple differential equation relative to the pressure disturbance:

$$\frac{1}{r}\frac{\partial}{\partial r}\frac{r}{\rho_0\bar{\omega}^2}\frac{\partial p}{\partial r} - \left(\frac{\alpha^2}{\rho_0\,\bar{\omega}^2} + \frac{n^2}{\rho_0 r^2\bar{\omega}^2} - \frac{1}{\gamma P_0}\right)p = 0 \tag{18}$$

where $\bar{\omega} = \omega - \alpha U$. This equation is solved under finiteness condition at $r = 0$ and under condition of $p \sim H_n^{(1)}(i\lambda r)$ at $r \to \infty$, where $H_n^{(1)}$ is Hunkel function of the n-th order of the first kind, $\lambda = \sqrt{\alpha^2 - \omega^2/c_0^2}$, $c_0 = \sqrt{\gamma P_0/\rho_0}$ is the sound velocity outside the jet and the cuts of function $\lambda(\alpha)$ are determined in such a way, that $\mathrm{Re}\,\lambda > 0$ over the whole list of Rieman's surface (this corresponds to p decrease at $r \to \infty$).

A solution of the spectral task (18) is local wave-number α and eigen-function $p(r)$ in each jet cross-section $z = const$, that is longitudinal coordinate z enters the equation (18) as a parameter. However, solution of Eq.(18) is not sufficient for determining the instability wave even in the main approximation. The point is, that the solutions of spectral task (18) are determined with the accuracy up to arbitrary multiplier $A(s)$. To relate the amplitudes $A(s)$ in different jet cross-section, the following approximation in terms of ε is used.

The terms of $O(\varepsilon)$ order in equations (13)-(16) give the so called solvability equation or, in other words, amplitude equation

$$I_1(s)\frac{d\,A}{d\,s} + I_2(s)A = 0 \tag{19}$$

where I_1 and I_2 are the integrals over the radial coordinate r from the terms p_0 and $\vec{v}_0$ of 0-th order in the expansion (17). The solution of Eq.(19) is expressed in the following form:

$$A(s) = A(0)\cdot \exp\left(-\int \frac{I_2}{I_1} ds\right) \tag{20}$$

The equation (20) connects the solutions of the spectral task (18) obtained in different jet cross-sections. This completely determines the shape of the instability wave in the jet.

In contrast to the internal region only one approximation in terms of ε should be obtained in the external region (outside the jet). In this approximation equations (13)-(16) are reduced to the wave equation in the static medium.

$$c_0^2 \nabla^2 p + \omega^2 p = 0 \tag{21}$$

With the use of Fourier transform in terms of the longitudinal coordinate, solution of this equation can be presented in the following form

$$p = \int_{-\infty}^{\infty} g(\eta) H_n^{(1)}(i\lambda r) \exp\left(\eta z + \frac{\pi}{2}\right) d\,z \tag{22}$$

$$g(\eta) = \int_{-\infty}^{\infty} Q(z) \exp(-i\eta z)\, d\,z \tag{23}$$

Equations (22)-(23) is a general form of the wave equation solution in the cylindrical coordinates and expresses the acoustic field outside the jet through density $Q(z)$ of the sources located on the jet axis. The source density $Q(z)$ determining the acoustic field outside the jet can be expressed through amplitude function $A(z)$ obtained as the result of the internal task solution. It was shown [27] that

$$Q(z) = A(z) \tag{24}$$

if the solutions of equation (18) are normalized in such a way, that $p_0(r, s) \to H_n^{(1)}(i\lambda r)$ at $r \to \infty$ in each jet cross-section.

The amplitude equation role in the method

We discuss now the amplitude equation role in the method considered. There are two aspects in this consideration. First, only the amplitude equation permits connecting the disturbance amplitudes in different jet sections. The wave packet has the following form

$$p = const\sqrt{\frac{1}{I_1(s)}}\cdot\exp\left(-\int_0^s \frac{I_0}{I_1} d\ s\right)\cdot\exp\left(i\int_0^s \alpha\ ds\right) \tag{25}$$

and is determined by three multipliers. The first two multipliers are determined by the amplitude equation and only the third one is determined by the imaginary part of wave number α. To solve equations (18) describing the disturbances in different jet sections such a normalization is chosen in the present work, that for each jet section $P = H_n^{(1)}(i\lambda r)$ in the region outside the jet. However since equations (18) are linear any other normalization could be chosen for their solutions. The normalization change is automatically taken into account through change of integrals I_0 and I_1 in amplitude equation (19). Due to complexity of amplitude equation, two first multipliers containing the integrals I_0 and I_1 are often omitted to simplify Tam's method [28-30]. This means that the wave packet is presentation in the form $p = \exp(i\int \alpha dz)$. In this case wave packet form will depend on the normalization of equation (18) solutions, i.e. the solution becomes absolutely arbitrary, in essence.

The second aspect in the amplitude equation role is the quantitative effect of the amplitude equation on the wave packet form and, hence, the radiation directivity. To evaluate this effect the predictions were made in which the amplitude equation was not solved and the wave packets were presented in the form of $p = \exp(i\int \alpha dz)$. It will be shown that without amplitude equation the prediction does not match to the experiment data. Really, the phase velocity of the wave in the maximum point is decrease as *Sh* increase (Fig.11b) but in experiment the maximum is displaced in upstream direction (Fig.11a).

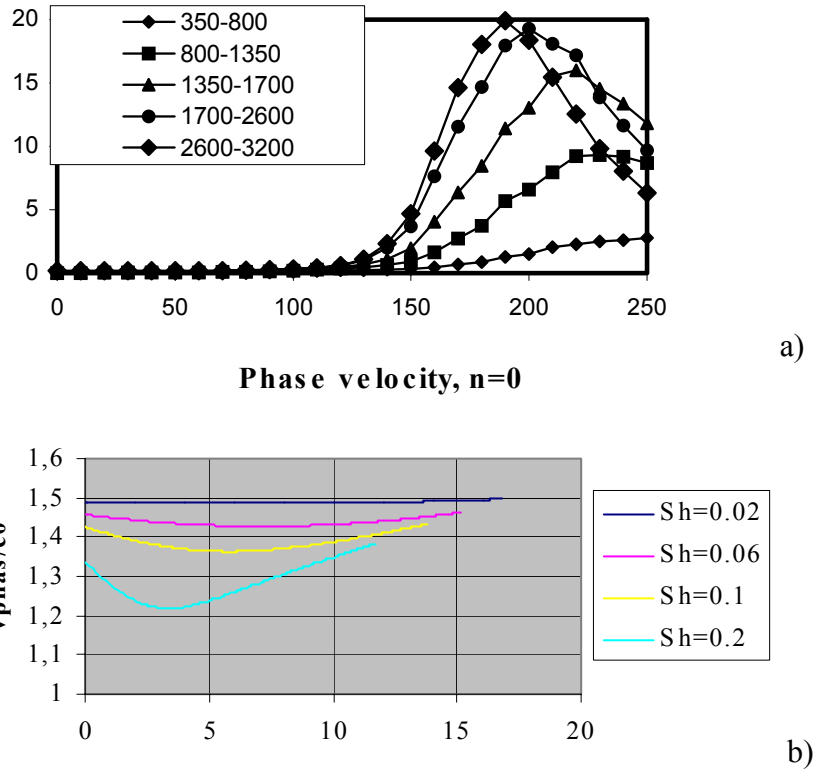

Figure 11. Measurements of axisymmetrical azimuthal mode in jet noise a) and decreasing of phase velocity for . Displacement of maximum upstream as frequency increase.

DIRECT MEASUREMENTS OF NOISE AZIMUTHAL STRUCTURE

To exclude the noise sources not associated with the Tam's mechanism from experiment, special efforts were made [31]. First, the well shaped convergent-divergent axisymmetrical nozzle designed for exit Mach number M=2 was fabricated. The notion of a "well shaped nozzle" included the requirement of flow uniformity at the nozzle exit as well as the property of velocity monotony on the nozzle wall, providing the boundary layer non-separation at any Reynolds numbers.

To avoid the appearance of shock-associated noise in the experiment (Fig.12), the design regime of issuing for well shaped nozzle was controlled with the use of visualization. Fig.13 presents the visualization results for fully expanded regime and under-expanded regime. The fine tuning of fully expanded regime was realized proceeding from the requirement of a complete absence of shocks in the jet. Due to the impossibility of simultaneous performance of the acoustic measurements and visualization on account of the interference introduced by optical equipment, the following scheme of the experiment was chosen. First, with the use of visualisation the necessary monitoring of the system of air supply, which assured the design issue regime, were chosen, and then the optical equipment was taken away from the anechoic chamber and the acoustic experiment was carried out.

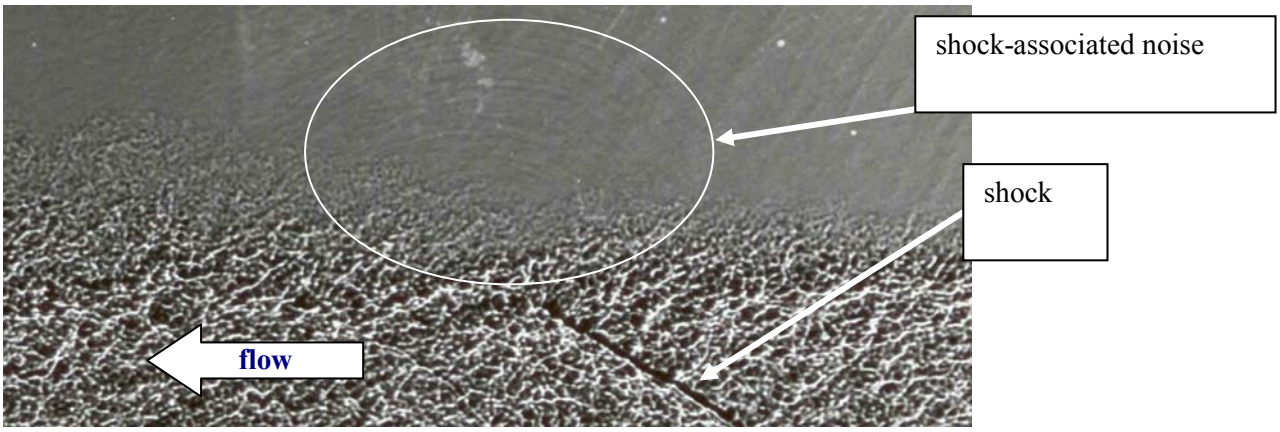

Figure 12. Fully expanded jet from conical convergent-divergent nozzle. Shock-associated noise component exists even for designed regime due to weak shocks structures in the jet (the shadowgraph was kindly given by Dr. V.G. Pimshtein). It was recently measured in azimuthal decomposition experiment (Kopiev, Zaitsev & Karavosov 2002).

a *b* *c*

Figure 13 Selected pictures from move: under-expanded (a,b) and fully expanded (c) regimes.

The technique of azimuthal decomposition of the sound field of supersonic jet with the use of a 6-microphone array (Fig.2) is described in detail in the review paper [7]. This technique gives a possibility of direct measuring the noise of each azimuthal mode separately. In experiment the mixing noise of

supersonic cold jet from convergent-divergent nozzles (d=3cm, d_{crit}=2.31cm) of design Mach number M=2.0 (it corresponds to jet velocity V=540 m/s, for cold jets the reservoir temperature equals to ambient temperature T~300°K) was studied. The experimental program consisted of measuring the azimuthal mode intensity in different frequency ranges by a six-microphone array. For acoustic measurements an array of ¼" ICP microphones (Bruel&Kjaer, type 4935) was used. These microphones provided good phase-matching characteristics. The microphone array moves along jet axis z from 0 to 240 cm. The signals from microphones were supplied to Dynamic Signal Acquisition Board NI4472. The nozzle orifice position corresponds to the section z=20 cm. The scheme of the experiment is presented in Fig.3.

Fig.15 presents the powers of three azimuthal modes a_0^2, a_1^2, a_2^2 (where subscript corresponds to the number of azimuthal harmonic) as the result of azimuthal noise decomposition. We see that only axisymmetric radiation dominates in the low frequency range. So, only a few first azimuthal modes give a contribution to the round jet noise. The second and the third modes are small in this range. The peak in axisymmetrical (n=0) mode directivity displaced upstream as Strouhal number increase. We present only low frequency results for jet noise azimuthal decompositions up to St~0.3.

The local Mach number in a jet was calculated from the data obtained with the use of stagnation pressure tube behind the normal shock and the data from static pressure probe before the shock (Fig.14) accordingly known formula [32].

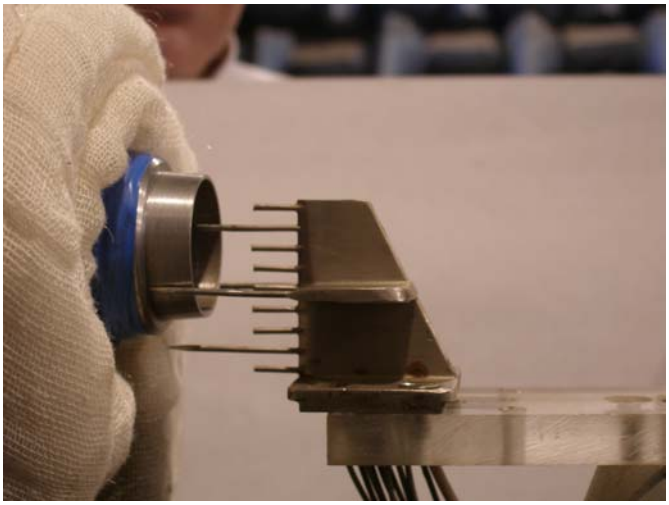

Figure 14. Mean flow measurements.

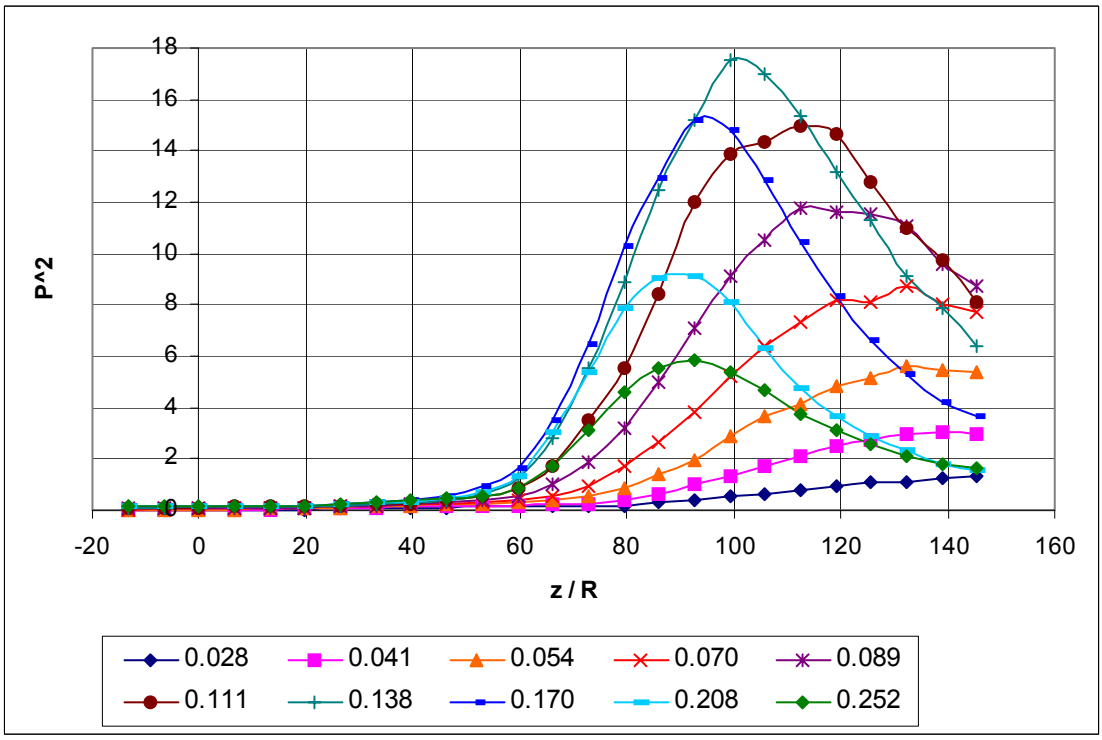
P^2
z / R
0.028
0.041
0.054
0.070
0.089
0.111
0.138
0.170
0.208
0.252

a)

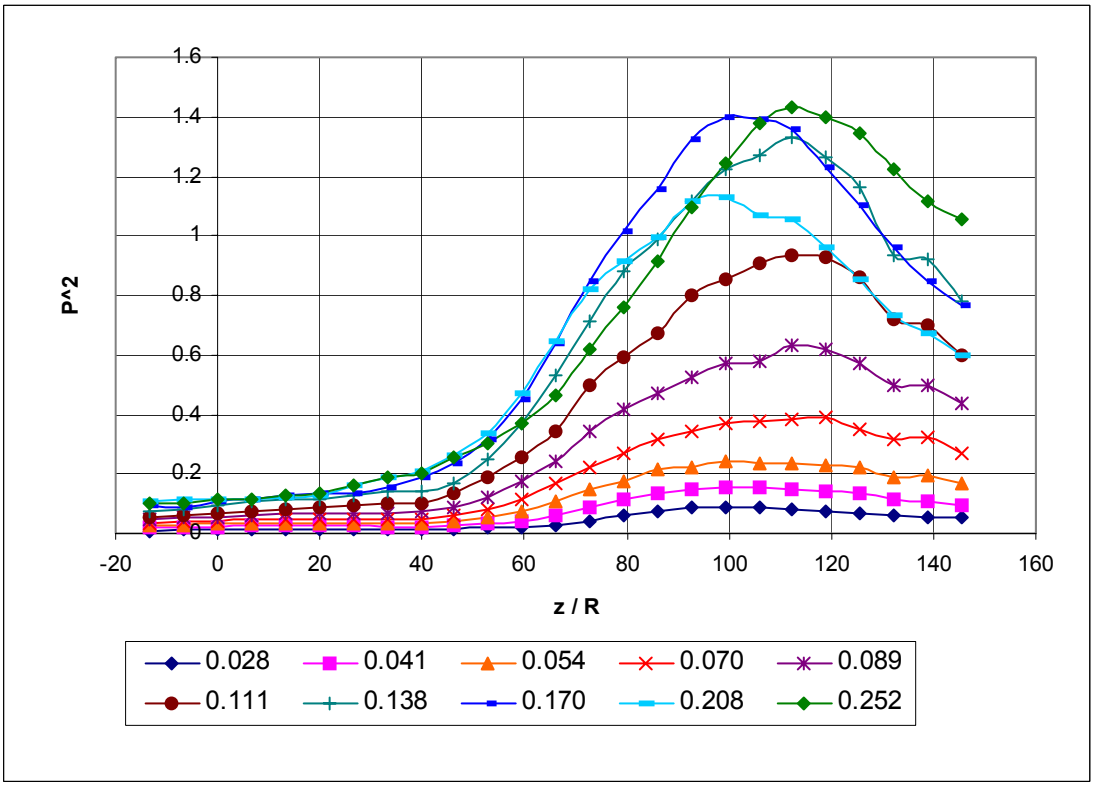
P^2
z / R
0.028
0.041
0.054
0.070
0.089
0.111
0.138
0.170
0.208
0.252

b)

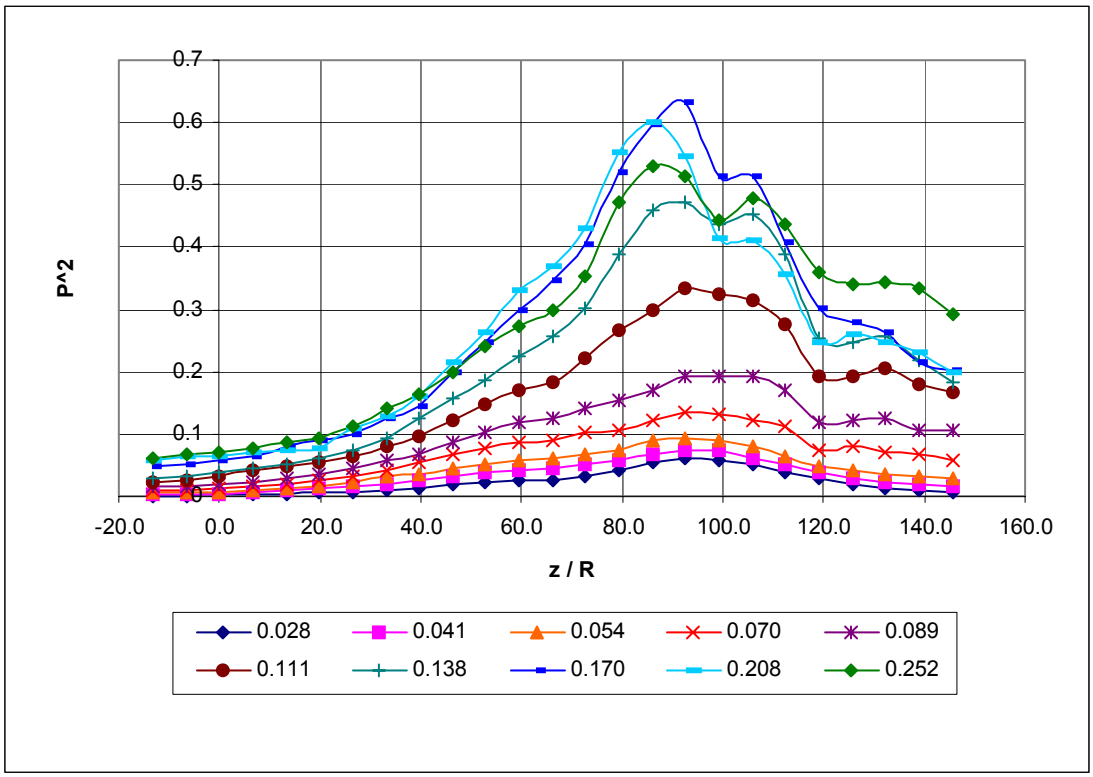

c)

Figure 15. Measured acoustic pressure level in different frequency ranges for harmonics a) *n*=0, b) *n*=1, c) *n*=2. Harmonic $n = 0$ contributes most of all in total pressure level.

Mean flow parameters underline the acoustic pressure prediction

The mean flow in the program was specified with the use of analytical expressions and for obtaining the non-steady disturbances the numerical solution of differential equations was made. The axial component of the mean flow velocity was determined as follows:

$$U = U_0, \quad \mathrm{r} < \mathrm{H}$$

$$U = U_0 \exp\left[-\frac{\ln 2}{B^2}(r - H)^2\right], \quad \mathrm{r} > \mathrm{H}$$

where U_0 is the velocity on the jet axis, B is the half-width of the mixing layer, H is the jet core size in the initial size. Thus, the axial velocity in the mean flow was determined by three functions: $U_0(z), B(z), H(z)$ where z is the longitudinal coordinate, which were calculated using the semi-empirical theory described in the handbook [32]. A comparison of measured and calculated velocity at the axis of the jet is presented in Fig.16. The temperature field in the mean flow was specified using Crocco-Busemann's equation and the radial component of the velocity in the mean flow was found from the equation of continuity.

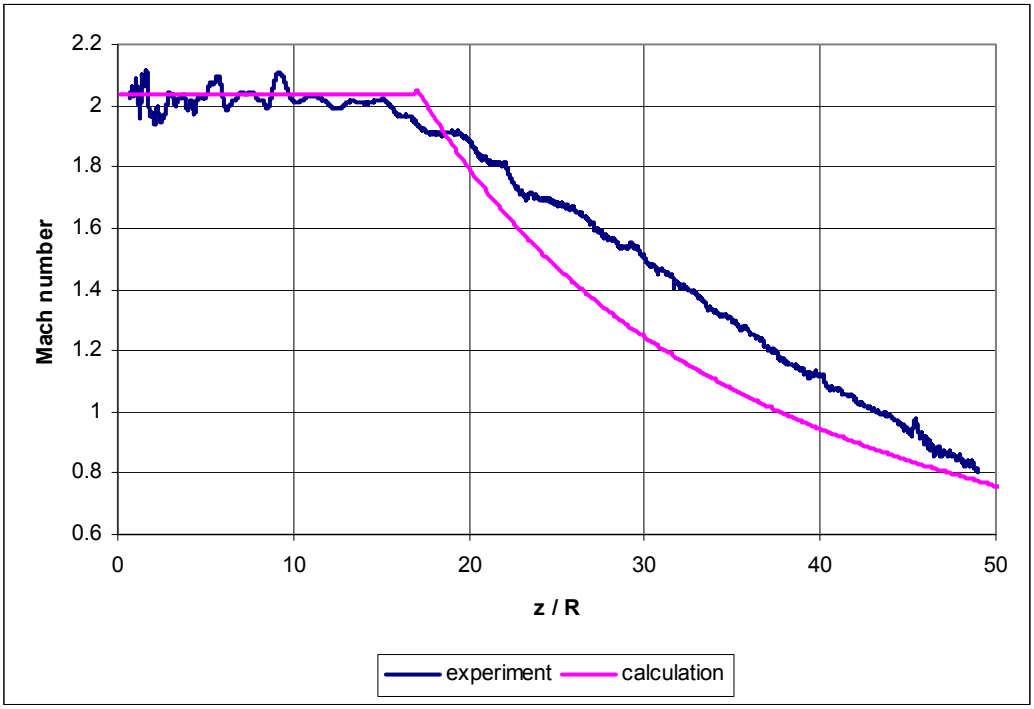

Figure 16 Comparison of measured and calculated mean flow axial velocity at the axis of the jet.

PREDICTION AND MEASUREMENT COMPARISON

The measurement results for well shaped nozzle are compared with the theory predictions. For predicting the jet near field the numerical program was worked out based on the instability wave theory considered above. For comparing with the predictions, the results of acoustical measurements in three frequency ranges were chosen for three azimuthal harmonics $n = 0, n = 1$ and $n = 2$. It is seen in Fig.17, where the measurement data are presented, that the largest contribution in the sound pressure level over all the frequency ranges is given by harmonic $n = 0$, a less contribution is given by harmonic $n = 1$ and still less contribution is given by harmonic $n = 2$. According to this observation, the most significant in the prediction and measurement comparison is harmonic $n = 0$.

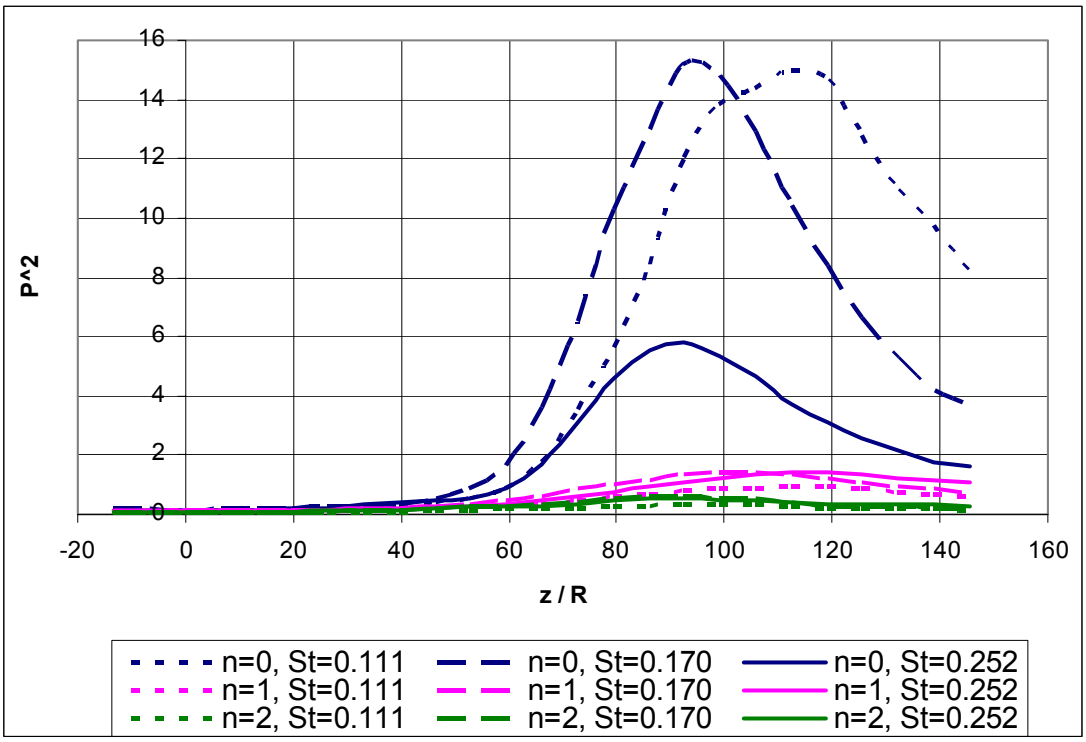

Figure 17. Measured acoustic pressure level in three frequency ranges for harmonics *n*=0, *n*=1 and *n*=2. Harmonic $n = 0$ contributes most of all in total pressure level.

Fig.18-21 presents a comparison between the prediction and measurement data related to acoustic radiation of a cold jet with $M = 2.04$ for three frequency ranges and three azimuthal harmonics. In doing so, its own normalization was chosen in each frequency range at which the radiation levels would coincide at the maximum point for predictions and measurements. Fig.22 presents relative values of pressure disturbances in the initial part of the mixing layer, corresponding to this normalization. According to the Tam's theory [2] the pressure disturbances near the nozzle edge is a white noise in time and space (in the azimuthal direction). In this case the pressure disturbance level in this region must be the same for different harmonics and frequency ranges. It is seen in Fig.22 that this value varies in dependency on harmonics and frequency. Nevertheless, this variation can be considered is rather small as compared with the dispersion of near field acoustic pressure (Fig.17).

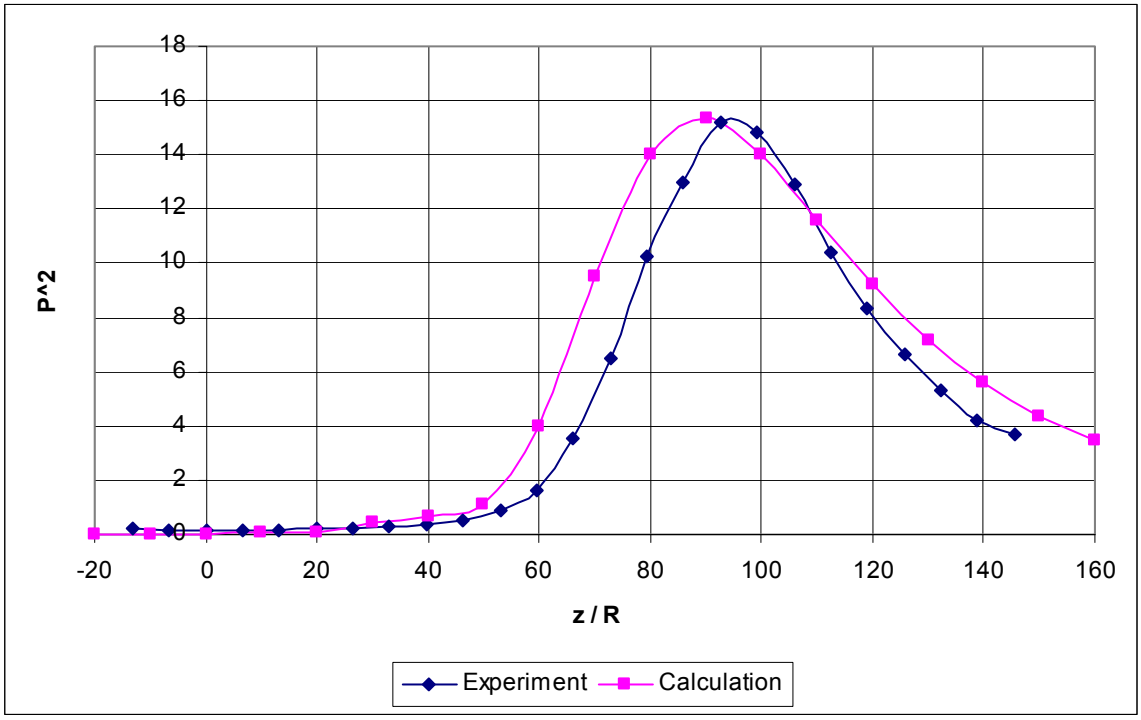

Figure 18. Comparison of the predicted and measured acoustic pressure levels. *n* = 0, St = 0.17.

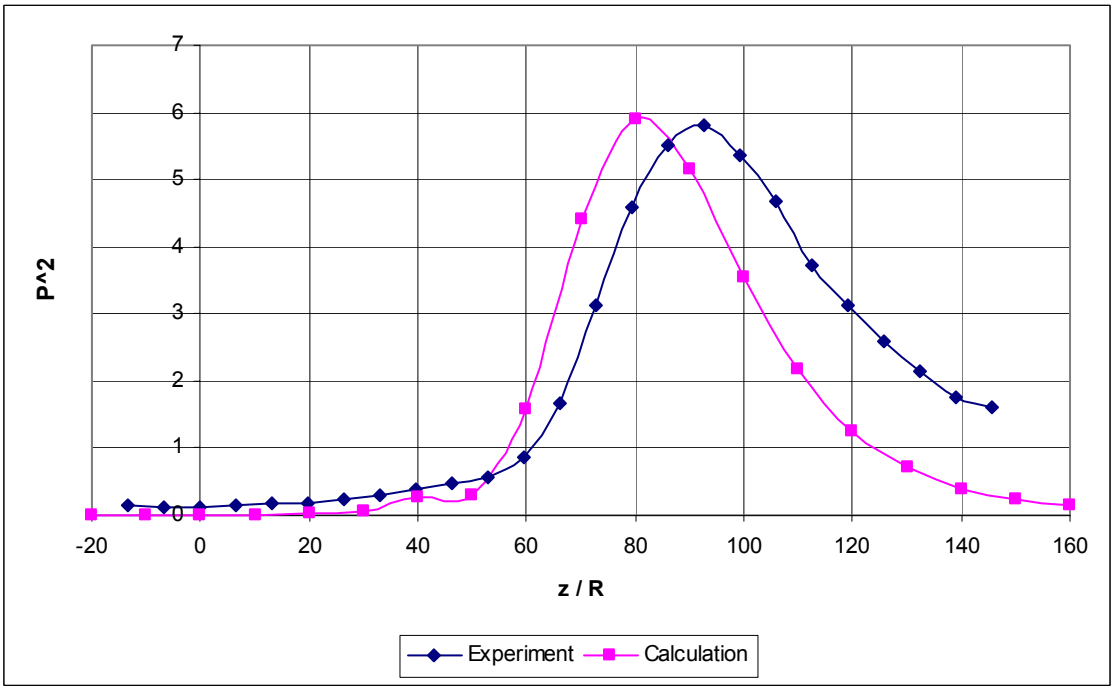

Figure 19. Comparison of the predicted and measured acoustic pressure levels. *n* = 0, St = 0.252.

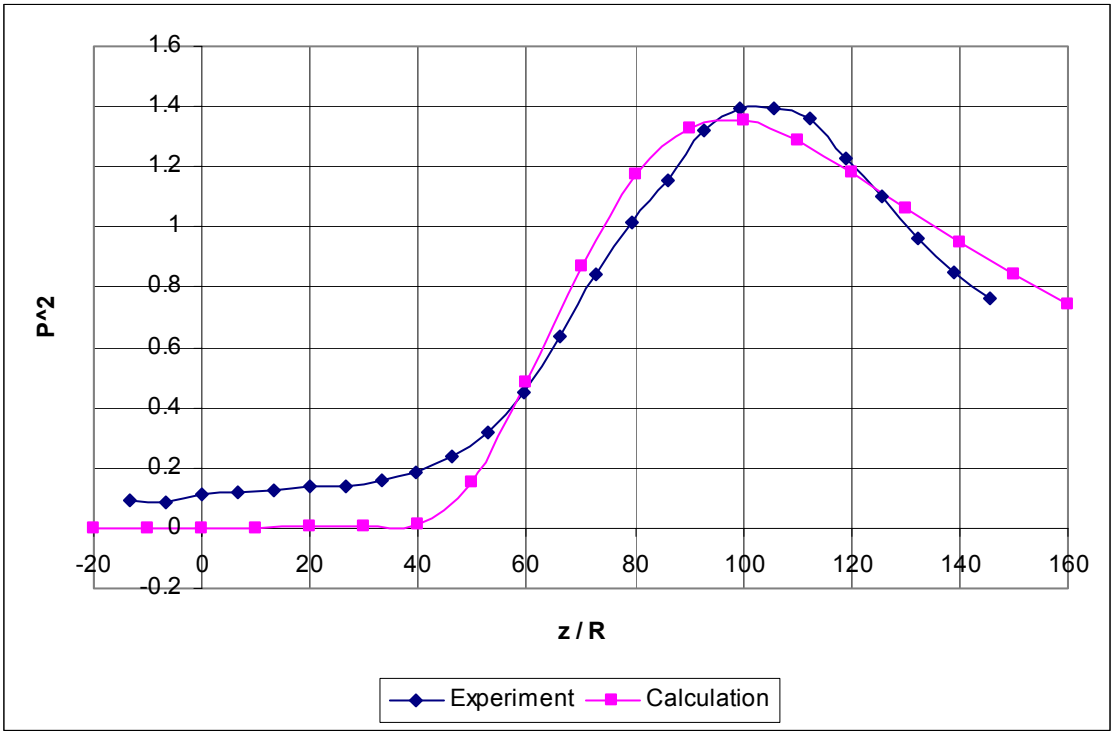

Figure 20. Comparison of the predicted and measured acoustic pressure levels. *n* = 1, St = 0.17.

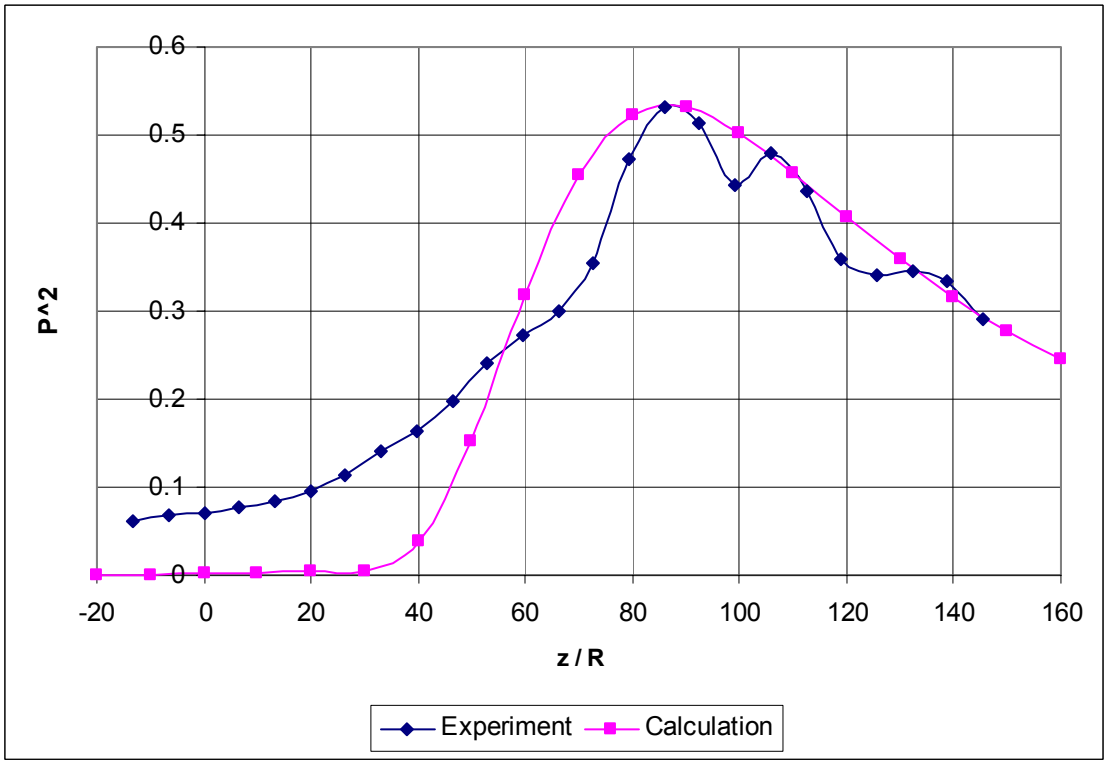

Figure 21. Comparison of the predicted and measured acoustic pressure levels.n = 2, St = 0.252.

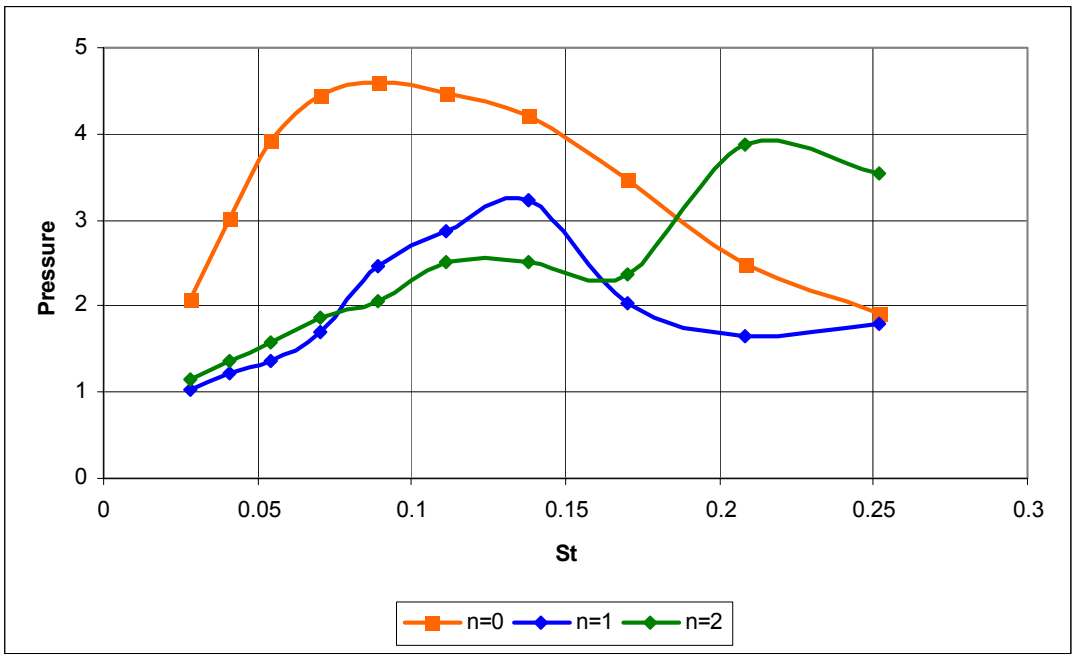

Figure 22. Relative values of pressure disturbances in the initial part of the mixing layer adjusted to acoustic measurements. Dispersion of these data is much less than near field acoustic level.

It follows from Fig.18-21 that the directivity characteristics predicted and measured are similar but the predicted peak of sound pressure is located more closely to the nozzle than in the measurements. This can indicate a less phase velocity in the instability wave or a larger extension of the radiation source in the real jet, in comparison with the numerical model. The most likely cause of this can be not very accurate description of the mean flow velocity profile in the initial jet part. The point is that integral I_0 (25) in many respects determining the wave packet form appears to be very sensitive to the velocity profile form [6]. At the same time it should be taken into account that the distance from the nozzle to the radiation peak location is twice as large as the distance from the jet axis to the measurement array. This means that the discrepancy of the peak locations $\frac{\Delta x}{R} = 10 - 20$ corresponds to the discrepancy in 2-4 degrees in the directivity pattern. Therefore there is a good reason to believe, as a whole, that the prediction results are in agreement with measurement data.

Consider the amplitude equation role on the wave packet form and, hence, on the radiation characteristics. To evaluate this effect the predictions were made in which the amplitude equation was not solved and the wave packets were presented in the form of $p = \exp(i\int \alpha dz)$ and compared with experiment and prediction accordingly full Eq. (25).

The wave packets in these prediction were of less extension and the radiation peak was closer to the nozzle than in the full predictions and even more so in the experiments. We see (Fig.7a) that in experiment the maximum in radiation directivity shifts upstream, as the frequency increases. Thus the calculation without amplitude equation is in disagreement with measurement data.

As a whole a conclusion is to be made that the amplitude equation is the essential part of the method and determines the solution in the main approximation.

PROSPECTS

We considered the instability wave model for high speed (supersonic) jet mixing noise. We discussed the verification of instability wave mechanism of noise radiation for supersonic jet. A comparison between the theory predictions and the measurement data shows that the instability waves are the real sources of noise generation in supersonic jet and their control means in fact the noise control.

Consider one possible strategy based on instability wave resonant coupling suggested in [31] which could have a direct importance for the flight vehicles future elaboration. For a round jet with a non-uniform mixing layer, all the Kelvin-Helmholtz eigen-modes are azimuthal harmonics, which are proportional to $\exp in\varphi$ and have an amplitude which varies in axial direction in a manner which can be ascertained in principle. Independence of each azimuthal harmonic from any other means that knowledge of the amplitude of a given harmonic, near the nozzle exit, entirely determines the amplitude of the wave packet and sound radiation by this harmonic. Given that, at least for $St < 0.3$, harmonics of high azimuthal numbers are poor sources of sound, we can conclude that total noise due to a non-uniform round jet is determined by the harmonics with small azimuthal numbers arising in the total disturbance near the nozzle exit.

The situation changes dramatically for a jet having a nozzle of a corrugated shape [31]. Clearly, the jet cross-section remains corrugated only for initial part of the jet. The effect of the mixing layer is to reduce the corrugation, ensuring that the jet cross-section becomes circular downstream. Nevertheless, even a weak corrugation, in the initial part of the jet, can strongly affect the disturbance behavior. It was shown that different azimuthal harmonics of a corrugated vortex sheet (an appropriate model for the initial part of a jet) are coupled. In other words, the eigen-modes consist not of a single harmonic but of a mixture of different harmonics (similarly two vibrators with weak coupling: if the eigen frequencies differ, then the weak coupling does not change the eigen forms, Fig.23a, but if the eigen frequencies are close to each other then the weak coupling leads to resonant interaction and strongly changes the shapes of eigen oscillations). Thus, in the case of resonant coupling, this mixture includes two different harmonics in the first approximation in corrugation parameter, a so-called strong mixture of two harmonics.

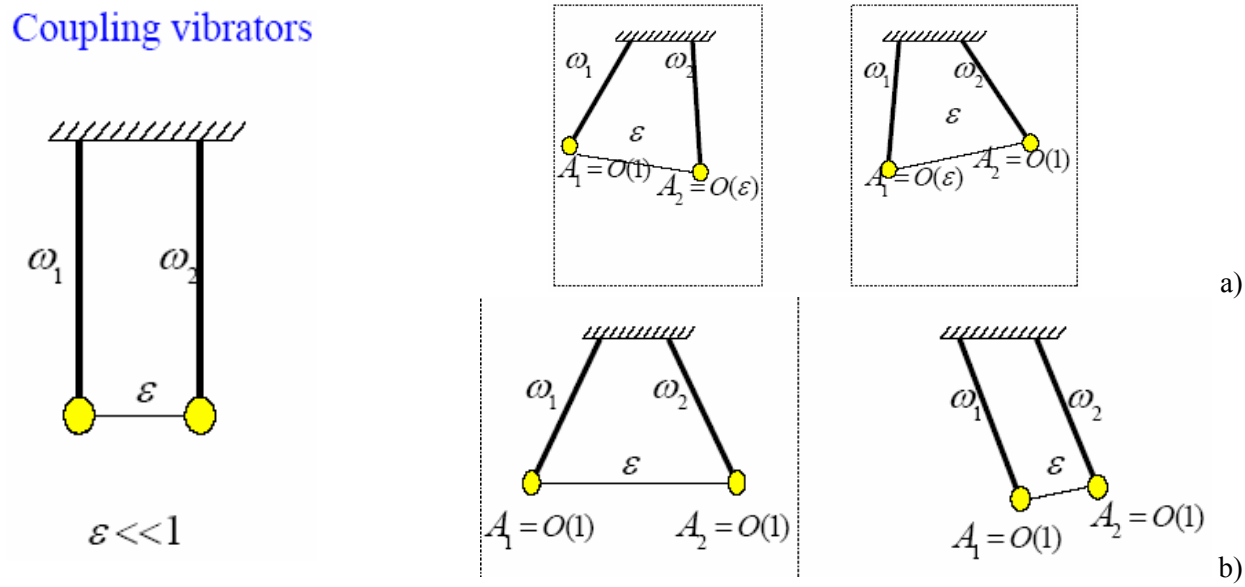

Figure 23. Coupling vibrators

For example, for a corrugated jet with a lobe number $s = 8$ the 1st and the 7th harmonics are in resonant coupling. It means that there are two abnormal spatial instability eigen-waves within such a jet. Each of

them is a strong mixture of the 1st and the 7th harmonics in the initial part of the jet. However, by the point at which the cross-section of the jet has becomes circular, one of them will have become a pure 1st harmonic whilst the other will have become a pure 7th harmonic. Note, that the latter eigen-mode is not an effective source of sound.

Thus, an excitation of the disturbances near the nozzle exit in the form of the 1st harmonic generates not one instability wave, as in the case of round jet, but two abnormal instability waves. They combine to give only the 1st harmonic at the nozzle exit cross-section and in some combination of the 1st and 7th harmonics downstream (where the later is non radiating, Fig.24).

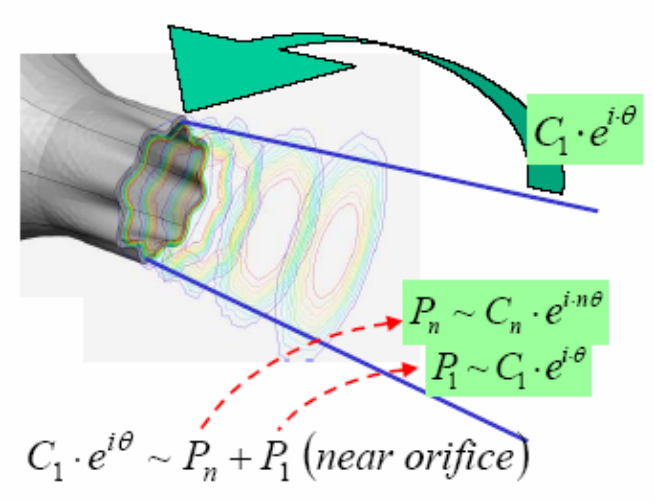

Figure 24 Transformation of radiating part into non radiating one

Hence, the splitting of the initial disturbance into two eigen-oscillations leads to the situation where part of the initial disturbance is transformed into a non-radiating mode. Moreover, if the initial disturbance is made up of a mixture of the first and the seventh harmonics exactly corresponding to the seventh eigen-oscillation for a corrugated vortex sheet, then such an initial disturbance completely transforms downstream into the seventh azimuthal harmonic and will not radiate at all.

The question related to preparing a required mixture of azimuthal harmonics in the nozzle exit plane and the role of chevrons, or other distortions, in solving this task are left to future investigations.

ACKNOWLEDGEMENTS

The authors would like to express his deep gratitude to Drs. S.A. Chernyshev, M.Yu. Zaitsev and N.N. Ostrikov for fruitful discussions. The work is partly realized with the support of Russian Foundation of Basic Research (RFBR 05-01-00670, 05-01-08052ofi_a)

REFERENCES

[1] Tam, C. K. W. “Jet Noise Generated by Large-Scale Coherent Motion” in “Aeroacoustics of flight vehicles. Theory and practice” ed. H. Hubbard, v. 1, pp. 311-390 ASA/AIP, 1991

[2] Tam, C.K.W. & Chen, P. (1979) A statistical model of turbulence in two-dimensional mixing layers. J Fluid Mech., Vol. 192, pp. 303-306.

[3] Ffowcs Williams J.E., Maidanik G. The Mach wave field radiated by supersonic turbulent shear flow. J. of Fluid Mech., 1965, v.21, p.641-657

[4] Bailly C., Candel S., Lafon P. Prediction of supersonic jet noise from a statistical acoustic model and a compressible turbulence closure. J. of Sound and Vibr. 1996, v.194 (2), 219-242

[5] Troutt T.R., Mc Laughlin D.K., "Experiments on the flow and acoustic properties of a moderate Reynolds number supersonic jet", ", J. Fluid Mech., 116, 123 – 156 (1982).

[6] V.F. Kopiev, S.A. Chernyshev, M.Yu. Zaitsev, V.M. Kuznetsov, Experimental validation of instability wave theory for round supersonic jet, 2006, AIAA-2006-2595

[7] Kopiev V.F., "Azimuthal decomposition of turbulent jet noise and its role for diagnostics of noise sources", VKI Lecture Series 2004-05 "Advances in Aeroacoustics and Applications", 2005, VKI.

[8] Kopiev V.F., Zaitsev M.Yu., Karavosov R.K. On azimuthal structure of supersonic jet noise. Proceedings of Tenth International Congress of Sound and Vibration ICSV10, Stockholm, Sweden, 2003, v.2, p.637-644

[9] J.W. Miles. On the reflection of sound an on interface of relative motion. JASA, 1957, v.29, N2, p. 226-228.

[10] H.S. Ribner. Reflection, transmission and amplification of sound by a moving medium JASA, v.29, 1957, N4, p. 435-441.

[11] J.W. Miles. On the disturbed motion of a plane vortex sheet. 1958, J. Fluid Mech., v. 4, p.538-552.

[12] P.A. Sturrock. Kinematic of growing waves. Phys. Rewiew,1958, v. 112, N 5, p. 1488-1503.

[13] R.J. Briggs. Electron-Stream interaction with plasmas. MIT, Cambridge, 1964.

[14] G. Birkhoff. Helmholtz and Taylor instability. Proc. Symp. App. Math. Soc. v. 13, p. 55-76, 1962.

[15] K.M. Case. Hydrodynamic stability and the initial value problem. Proc. Symp. Appl. Math. Am. Math. Soc. v. 13, 1962, p.25-33.

[16] P.N. Shankar. On the evolution of disturbances at an inviscid interface. 1981, J. Fluid Mech. v. 108, p. 159-170.

[17] R.D. Richtmyer Principles of advanced mathematical physics. V.1, Springer 1978.

[18] P. Gottlieb. Sound source near a velocity discontinuity. JASA, 1960, v. 32, N9, p. 1117-1122.

[19] M.S. Howe. Transmission of an acoustic pulse through a plane vortex sheet. 1970. J. Fluid Mech. v. 43, p. 353-367.

[20] C.K.W. Tam Directional acoustic radiation from a supersonic jet generated by shear layer instability. J. of Fluid Mech., 1971, v.46, p.757-768.

[21] N. Hardisity. The instability due to acoustic radiation striking a vortex sheet on a subsonic stream, Proc.R.Soc Edinborough (a), 1973, v.71, p. 141-149.

[22] M.A. Mironov. Effect of periodical volume source on the flow with 2D tangential discontinuity. Acoust. Zhurn (translated in Acoust. Phys), 1975, v.21, n1, p.79-85.

[23] Howe M.S. A review of the theory of trailing edge noise. J. Sound Vib. 1978, v.61, 437-465

[24] Crighton D.G. The Kutta condition in unsteady flow. Ann.Rev. Fluid Mech, 1985, v.17, 411-445

[25] Tam, C.K.W. & Burton, D.E. (1984) Sound generated by instability waves of supersonic flows: Part1. Two-dimensional mixing layers. J. Fluid Mech., Vol. 138, pp. 249-272.

[26] Tam, C.K.W. & Burton, D.E. (1984) Sound generated by instability waves of supersonic flows: Part2. Axisymmetric jets. J. Fluid Mech., Vol. 138, pp. 273-295.

[27] Tam C.K.W., Chen P. Turbulent mixing noise from supersonic jets. AIAA Journal, vol. 32, No. 9, p. 1774-1780, 1994.

[28] Millet C., Casalis G., Selection of acoustic modes in the vicinity of supersonic jets. AIAA paper 2002-2452, p. 1-7

[29] Morris, P.J. & Bhat, T.R.S. (1993) Supersonic elliptic jet noise. AIAA Paper 93-4409

[30] Kopiev V.F., Ostrikov N.N., Chernyshev S.A., Elliot J.W., “Aeroacoustics of supersonic jet issued from corrugated nozzle: new approach and prospects”, International Journal of Aeroacoustics, 2004, 3 (3), pp. 199-228

[31] Abramovich G.N. Applied gas dynamics. Moscow, Nauka, 1969, 824p.